55
1-15-92 JS (2)

PREPARED FOR THE U.S. DEPARTMENT OF ENERGY,
UNDER CONTRACT DE-AC02-76-CHO-3073

PPPL-2802
UC-420, 421, 426

PPPL-2802

COMPARISON OF MEASURED ELECTRON DENSITY RISE AND CALCULATED NEUTRAL BEAM PARTICLE DEPOSITION IN THE TFTR TOKAMAK

BY

H. PARK ET AL.

December 1991

PPPL PRINCETON PLASMA PHYSICS LABORATORY

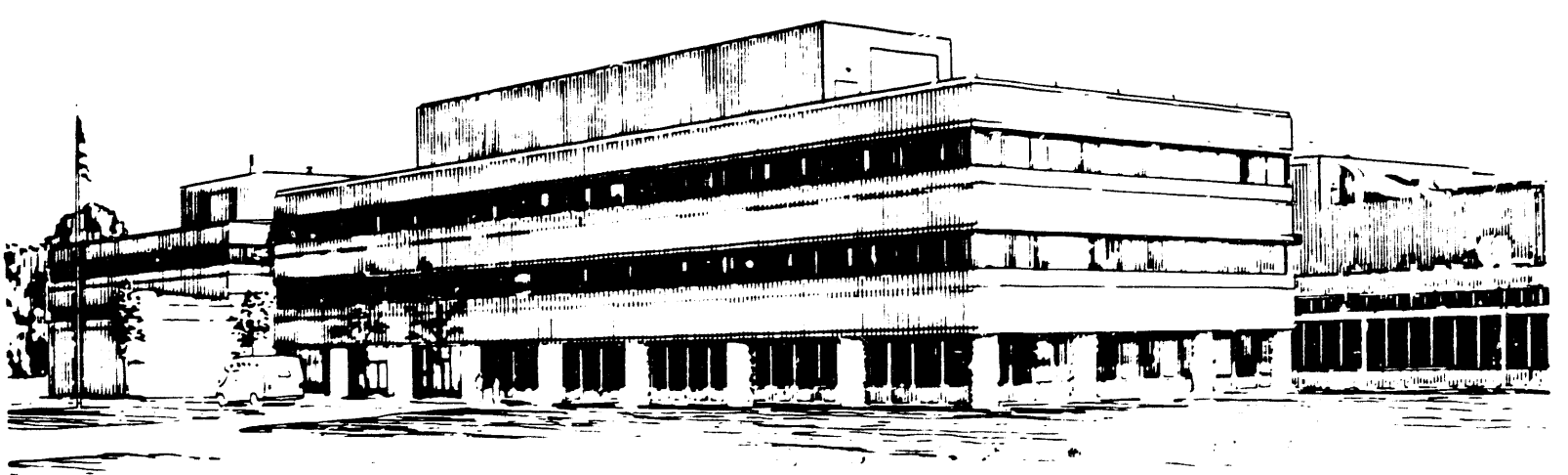

PRINCETON UNIVERSITY, PRINCETON, NEW JERSEY

NOTICE

This report was prepared as an account of work sponsored by an agency of the United States Government. Neither the United States Government nor any agency thereof, nor any of their employees, makes any warranty, express or implied, or assumes any legal liability or responsibility for the accuracy, completeness, or usefulness of any information, apparatus, product, or process disclosed, or represents that its use would not infringe privately owned rights. Reference herein to any specific commercial produce, process, or service by trade name, trademark, manufacturer, or otherwise, does not necessarily constitute or imply its endorsement, recommendation, or favoring by the United States Government or any agency thereof. The views and opinions of authors expressed herein do not necessarily state or reflect those of the United States Government or any agency thereof.

NOTICE

This report has been reproduced directly from the best available copy.

Available to DOE and DOE contractors from the:

Office of Scientific and Technical Information
P.O. Box 62
Oak Ridge, TN 37831;
Prices available from (615) 576-8401.

Available to the public from the:

National Technical Information Service
U.S. Department of Commerce
5285 Port Royal Road
Springfield, Virginia 22161
703-487-4650

PPPL--2802

DE92 005131

Comparison of Measured Electron Density Rise and Calculated Neutral Beam Particle Deposition in the TFTR Tokamak

H. K. Park, C. W. Barnes*, R. Budny,

D. McCune, G. Taylor, and M. C. Zarnstorff

Princeton Plasma Physics Laboratory,

Princeton University, Princeton, NJ 08543

Abstract

The initial rate of rise of the central electron density during $\sim$ 100 keV deuterium neutral beam injection is found to agree well with calculations of the beam deposition rate. The best agreement is with beam deposition calculations using older tabulations of the atomic cross-sections; the effects of using new tabulations or including multi-step ionization processes appear to approximately cancel. The neutral-beam deposition profile is a strong function of both the magnitude and the shape of the target plasma density. Peaked heating profiles can be achieved at high target densities only from peaked target density profiles.

---

* Los Alamos National Laboratory, Los Alamos, NM

MASTER

Precise information on the neutral-beam deposition profile is essential to the study of neutral-beam-heated tokamak plasmas, since the beam deposition profile provides the basis for understanding particle and heat transport experiments. It is also important to know how to create peaked deposition to optimize the effect of heating. In the past, the determination of the deposition profile primarily relied on computations. Recent studies[1,2] have re-examined various atomic cross-sections and reported results which deviated from older measurements.[3-5] In this paper, the measured rate of rise of the electron density in TFTR is compared to the calculated electron source rate from neutral-beam injection, $[S_{be}(r,t)]$. The good agreement in the center of the discharge supports the use of the deposition calculations, and allows further comparison to different atomic cross-sections and processes. The shape of the beam deposition profile is found to depend not only on the magnitude but also the shape of the target plasma density for the TFTR tangential injection system.

A time-dependent transport code, TRANSP,[6,7] is used to calculate the electron production rate, employing a Monte Carlo calculation for the beam ions and neutrals. In this calculation, the measured time evolution of $T_{e,i}(r)$, $n_e(r)$, $Z_{eff}(r)$, and wall recycling via H_α are used. The deuterium neutrals from the neutral beam produce electrons through several different processes. The code calculates electron production by the basic processes: electron-impact ionization, proton-impact ionization, and ionization and charge exchange processes with impurities. The ionization of the thermal neutrals produced by charge exchange beam deposition are also calculated.[8] A unique feature of TRANSP is the inclusion of beam deposition from interaction with other beam ions and calculation of the beam charge exchange recapture process. The important features of a beam species mix, beam divergence, and power profile across the beam source are accurately modeled in this calculation. The estimated error in the TRANSP calculation of the local electron source rate due to the beams is $\pm 10\%$. The uncertainty is largely due to Monte Carlo numerical noise. TRANSP calculations can be performed with both the old 3-5 (σ_1) and new 1,2 (σ_2) tabulations of the atomic

physics cross-sections for the same discharge and compared with the experiments. Multi-step ionization[9,10] (MSI), a process which effectively enhances the cross-sections, is important in plasmas where the density is high. The effect of MSI processes was previously examined in the TFR[11] tokamak. There, the heating-beam deposition was examined through shine-through measurements. In general, the measured shine-through power was less than the calculation with σ_1. When the MSI processes were included, the measured shine-through power was more than the calculation. At present, the MSI calculation is available only with σ_1 through the models of Refs. [9] and [10].

An increase in local electron density can be the result of changes in the electron particle source from either neutral beam deposition or recycling neutrals from the tokamak wall. At the center of the plasma, the electron density is least affected by wall recycling changes[12] during the initial period (the first 100 msec) of neutral beam injection. Thus, provided that the changes in the density can be measured with sufficient accuracy, the initial central density rise provides a good test of deposition calculation.

The deuterium plasmas studied had a wide range of parameters: the toroidal magnetic field B_T was varied over the range 4–5 T, the plasma current I_P over 1–2 MA, and the heating power P_{be} over 5–22 MW. In TFTR, twelve neutral beams inject tangentially, with six co-tangential to the plasma current and six counter-tangential. Deuterium neutral beams are injected with full energies of 90–110 keV. To reduce the effects of plasma rotation on the measured density or beam deposition, only discharges with nearly balanced momentum injection are studied, i.e., $|(P_{co} - P_{ctr})/(P_{co} + P_{ctr})| \leq 0.2$, where P_{co} and P_{ctr} are the powers of the neutral beams injected co-parallel and counter-parallel to the plasma current, respectively.

The time-dependent electron density is calculated by inversion[13] of the measured line-integral density along 10 chords. The calculation takes into account the elongation of the magnetic flux surfaces (as inferred from poloidal field measurements

outside the plasma) and a self-consistent Shafranov shift. The absolute and relative uncertainties in the determination of local electron density are $\pm$ 1.5 and 0.5×10^{18} m^{-3}, respectively. These uncertainties are constant across the profile.[14]

The calculated changes in electron density with σ_1 are compared to the measured values in Fig. 1. As shown in this figure, the initial rate of rise of the local electron density at small minor radii ($r/a \leq 0.5$) can be entirely explained by beam fueling. In the outer region of the plasma ($r/a \geq 0.5$) the particle influx from the wall quickly dominates the particle source.

The best agreement with the measured central electron density rise is obtained using σ_1. Among σ_2 points, the hydrogen impact ionization cross-section is significantly smaller at low energies compared to those of σ_1 points. This results in the calculations predicting deeper penetration and significantly more on-axis deposition. The σ_2 for electron ionization and charge exchange processes are relatively close to the σ_1.

The difference between the calculated rise ($\Delta n_e(0)_{cal}$) in the central electron density for the neutral-beam particle source and the measured rise ($\Delta n_e(0)_{meas}$) over the initial 100 msec, normalized to the measured value, is shown in Fig. 2. This difference is shown using σ_1, σ_1 with MSI processes, and σ_2. As expected, the effects of MSI processes and the differences in cross-sections are significant in plasmas with high density. Calculations including MSI processes with the σ_2 should provide the best results for comparing to the experiments. The relative effect of MSI processes in the calculations with σ_2 are expected to be similar to those with σ_1. Since the MSI processes enhance the cross-sections, while the new hydrogen impact ionization cross-sections are smaller, the effect of including the MSI processes and using σ_2 roughly cancel, and would be expected to result in agreement with calculations just using σ_1.

To compare deposition calculations for a number of conditions it is convenient to

define the deposition profile shape factor

$$H_{ne} = \frac{S_{be}(0,t)}{\langle S_{be}(r,t)\rangle}, \tag{1}$$

where $S_{be}(0,t)$ and $\langle S_{be}(r,t)\rangle$ are central and volume averaged electron source rate due to the neutral-beam, respectively. This definition is similar to the density peakedness factor $F_{ne} = n_e(0)/\langle n_e\rangle$, where $n_e(0)$ is the central electron density and $\langle n_e\rangle$ is volume-averaged electron density.

The penetration of the heating-beam is expected to be an exponential function of electron density. The calculated H_{ne} for a wide range of line-averaged densities ($\bar{n}_e$) with relatively broad profile shapes ($F_{ne} \leq 2$), can be described as

$$H_{ne} = a\ exp(-b\ \bar{n}_e) \tag{2}$$

where a and b are appropriate coefficients. In a plasma with a low target density, the differences between using σ_1 or σ_2 in the calculation are relatively small and effects of MSI processes are not significant. As the target density is increased, the effects of MSI and differences due to cross-sections are pronounced, but go in different directions. The calculated H_{ne}, using σ_1, σ_1 with MSI processes, or σ_2 is fitted to Eq. (2) and the coefficients are evaluated. The ratio of the calculated H_{ne} to the fitted H_{ne} is illustrated in Fig. 3. Here, the averaging time for the calculation of H_{ne} was 50 msec. For the TFTR plasmas, the e-folding values of $\bar{n}_e$ for H_{ne} with the σ_2 and σ_1 are 3.8 and $3.0 \times 10^{19}/m^3$, respectively. Thus the calculated penetration depth varies by $\cong 30\%$ due to the differences in atomic cross section tabulations. When the MSI processes are included in the calculation with σ_1, the penetration depth is reduced by $\cong 20\%$ and the corresponding e-folding value is $2.4 \times 10^{19}/m^3$.

However, H_{ne} for peaked profiles ($F_{ne} \geq 2$) deviates significantly from the exponential dependence projected for the broad target profiles. Figure 4 shows the ratio between the calculated H_{ne} for a variety of profile shapes and the fitted H_{ne}, calculated with σ_1 in Fig. 3. The penetration depth for peaked density profiles is significantly enhanced compared to that for broad profiles as $\bar{n}_e$ is increased in TFTR plasmas.

In neutral-beam heated tokamak plasmas, it is desirable to have a peaked deposition profile to optimize heating efficiency. A peaked H_{ne}, while not a sufficient condition, is helpful for improved energy confinement [15] in neutral-beam heated plasmas. In order to maintain a peaked H_{ne} at high density, the density profile has be peaked.

In summary, the calculated neutral-beam deposition in a tokamak plasma is consistent with the measured central electron density rise over a wide range of plasma density and profile shape. Use of the older atomic physics cross-section tabulation gives the best agreement, as the effects of the new tabulation of cross-sections or including multi-step ionization processes appear to cancel even at high density for TFTR parameters. However, the new tabulation of atomic cross-sections together with MSI processes should be used in the calculation of neutral beam penetration in plasmas. The beam deposition profile shape is not only a function of line density but also a strong function of the target density profile shape in a tangential injection system like TFTR. Obtaining strongly peaked heating profiles requires low target density or highly peaked targets, preferably both.

Acknowledgments

The authors wish to acknowledge valuable discussions with Drs. S.D. Scott and J.D. Callen and the assistence of R. Phaneuf. The authors wish to thank the TFTR staff, the Neutral Beam Group who contributed to the completion of this work. This work was supported by U.S. Department of Energy contract No. DE-AC02-76-CHO-3073.

References

[1] Shah, M.B., Elliott, D.S., Gilbody, H.B., J. Phys. B: At. Mol. Phys. **20** (1987) 2481-2485.

[2] Barnett, C.F., ORNL-6086, Vol-1, Controlled Fusion Atomic Data Center, ORNL, (July, 1990)

[3] Rudd, M.E., Kim, Y.K., Madison, D.H., Gallagher, J.W., Rev. Mod. Phys. **57** (1985) 965.

[4] Olson, R.E., Haselton, H.H., Phys. Rev. **A 16** (1977) 531.

[5] Riviere, A.C., Nucl. Fusion **11** (1971) 363.

[6] Hawryluk, R.J., in Physics of Plasma Close to Thermonuclear Conditions, edited by Coppi, B., *et al.* (Commission of the European Communities, Brussels, 1980), Vol. 1, p. 19.

[7] Goldston, R.J., McCune, D.C., Towner, H.H., *et al.*, Comput. Phys. **43** (1981) 61.

[8] Tamor, S.J., Compt. Phys. **40** (1981) 104.

[9] Boley, C.D., Janev, R.K., Post, D.E., Phys. Rev. Lett. **52** (1984) 534.

[10] Janev, R.K., Boley, C.D., Post, D.E., Nucl. Fusion **29** (1989) 2125.

[11] Equipe TFR, Plasma Phys. Controlled Fusion **29** (1986) 37.

[12] Mansfield, D.K., Efthimion, P.C., Hulse, R.A., *et al.*, in Plasma Phys. Controlled Fusion, Vol. IID, Part I, European Physical Society Meeting, Madrid (1987) 314.

[13] Park, H.K., Plasma Phys. Controlled Fusion **31** (1989) 2035.

[14] Park, H.K., Rev. Sci. Instrum. **61** (1990) 2879.

[15] Callen, J.D., Christiansen, J.P., Cordey, J.G., *et al.*, Nucl. Fusion **27** (1987) 1857.

Figures

Fig. 1. A comparison between the measured electron density and the calculated electron source from the neutral beams for several different radii. The target plasma has a low line-averaged density ($\bar{n}_e = 0.8 \times 10^{19}\ m^{-3}$), and $I_P = 1.4$ MA, $B_T = 4$ T, $P_{be} = 14$ MW and $a = 0.9\ m$. The histograms represent the integral of the calculated $S_{be}(r,t)$ from the start of beam injection at 4.0 sec.

Fig. 2. The normalized difference between calculated and measured initial central electron density rise is shown as a function of target plasma density for 6 different discharges, calculated with the three different methods; □ - with σ_2, ○ - with σ_1, and filled □ - with σ_1 and MSI processes. The time averaging was 100 msec and plasma parameters are as follow; B_T ranges over 4-5 T, I_P over 1-2 MA, and P_{be} over 10-22 MW.

Fig. 3. The ratio between the calculated and fitted H_{ne} is shown as a function of $\bar{n}_e$ for the broad target density profiles ($F_{ne} \leq 2$), H_{ne} is calculated by the three different methods; the symbols are the same as in Fig. 2 and each data set has then been fit separately. For the fitted data calculated with σ_2, a = 4.67 and b = $0.26\ m^{-3}$. For the fitted data calculated with σ_1, a = 4.76 and b = $0.33\ m^{-3}$. For the fitted data calculated with σ_1 together with MSI processes, a = 5.27 and b = $0.41\ m^{-3}$.

Fig. 4. The enhanced penetration of the heating-beam due to effects of the target density profile shape are illustrated. The ratio between the calculated H_{ne} for a variety of target density profile shapes and the fitted H_{ne}, calculated with the σ_1 for the broad profile shapes is depicted as a function of $\bar{n}_e$. Filled □ - $F_{ne} \leq 2$, ○ - $2.0 \leq F_{ne} \leq 2.5$, △ - $2.5 \leq F_{ne} \leq 3.0$, and filled ○ - $F_{ne} \geq 3.0$.

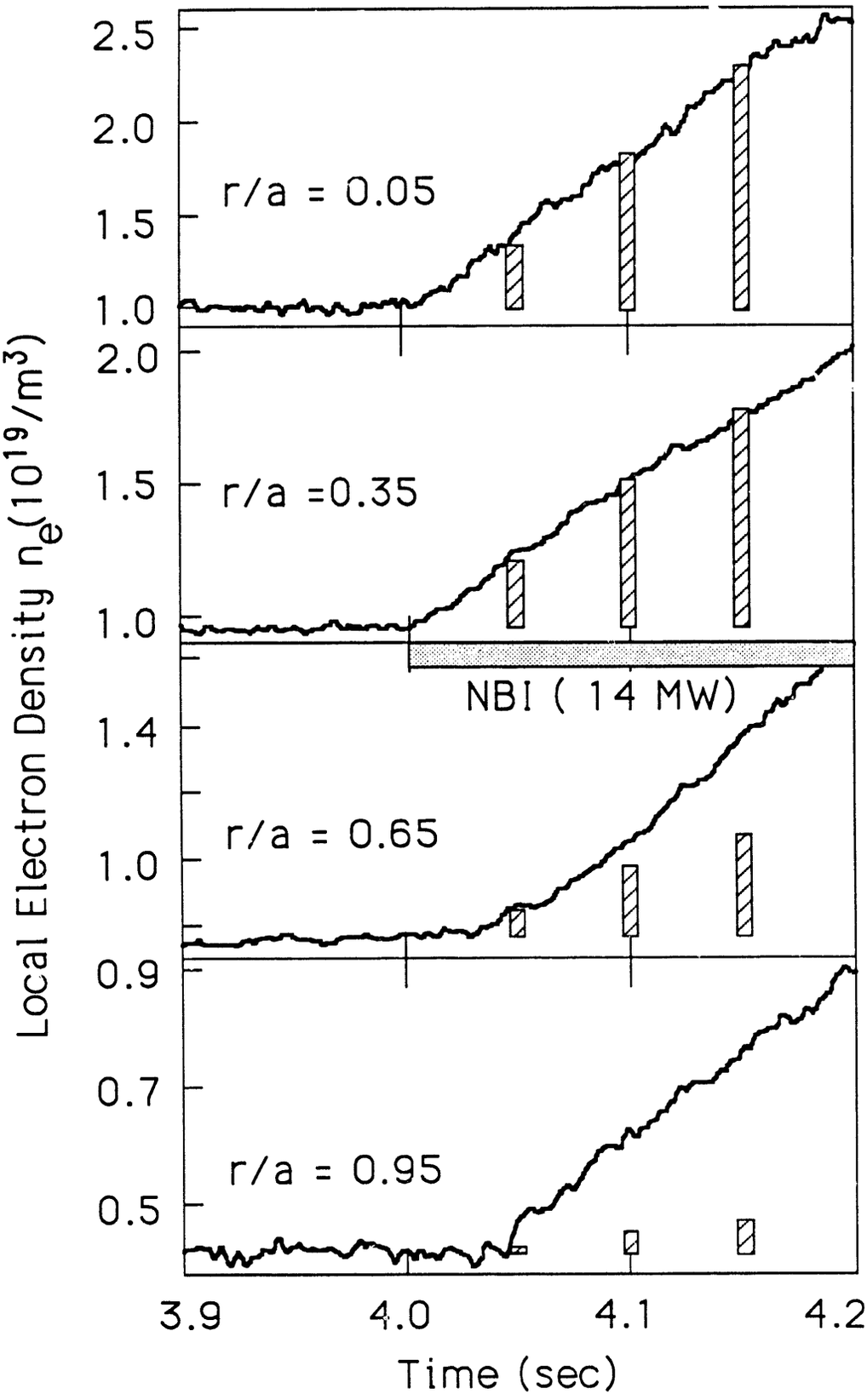
2.5
2.0
1.5
1.0
r/a = 0.05
2.0
1.5
1.0
r/a =0.35
NBI (14 MW)
1.4
1.0
r/a = 0.65
0.9
0.7
0.5
r/a = 0.95
Local Electron Density $n_e(10^{19}/m^3)$
3.9
4.0
4.1
4.2
Time (sec)

Fig. 1

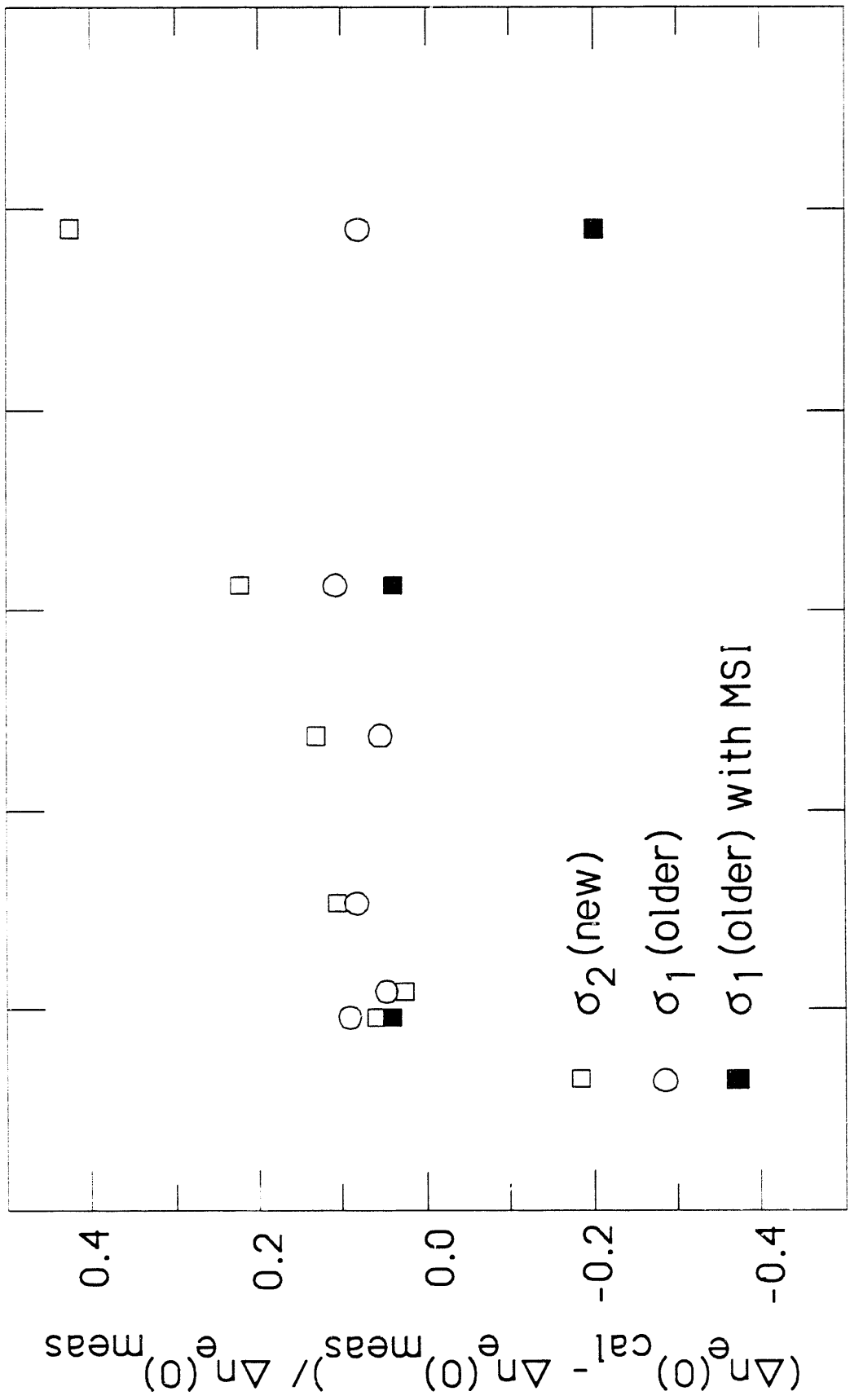
$(\Delta n_e(0)_{cal} - \Delta n_e(0)_{meas}) / \Delta n_e(0)_{meas}$
0.4
0.2
0.0
-0.2
-0.4
0
1
2
3
4
5
6
Target Density $(\overline{n_e})$ $(10^{19}/m^3)$
σ_2 (new)
σ_1 (older)
σ_1 (older) with MSI

Fig. 2

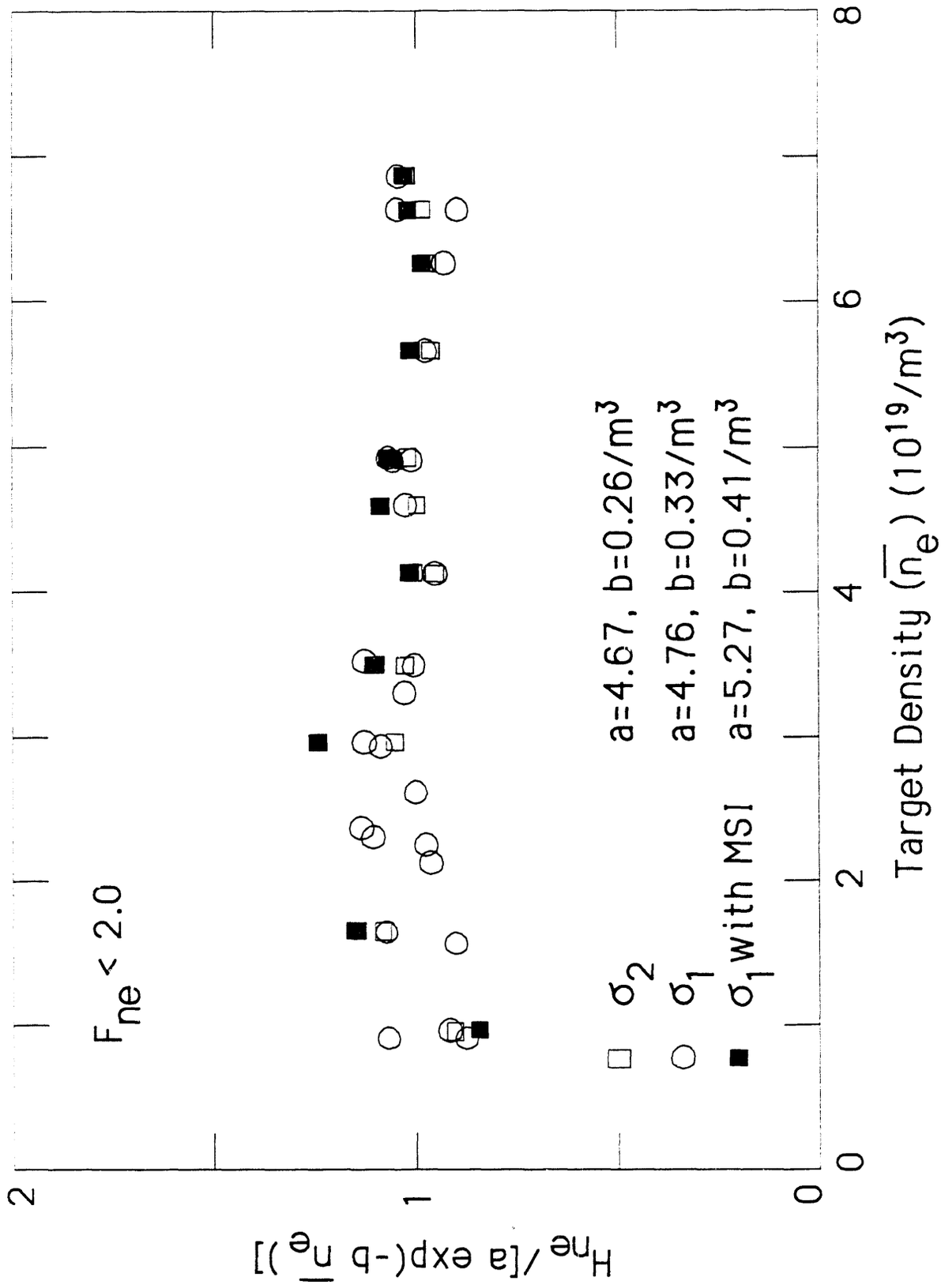
$H_{ne}/[a\ exp(-b\ \overline{n_e})]$
2
1
0
0
2
4
6
8
Target Density $(\overline{n_e})$ $(10^{19}/m^3)$
$F_{ne} < 2.0$
σ_2 a=4.67, b=0.26/m^3
σ_1 a=4.76, b=0.33/m^3
σ_1 with MSI a=5.27, b=0.41/m^3

Fig. 3

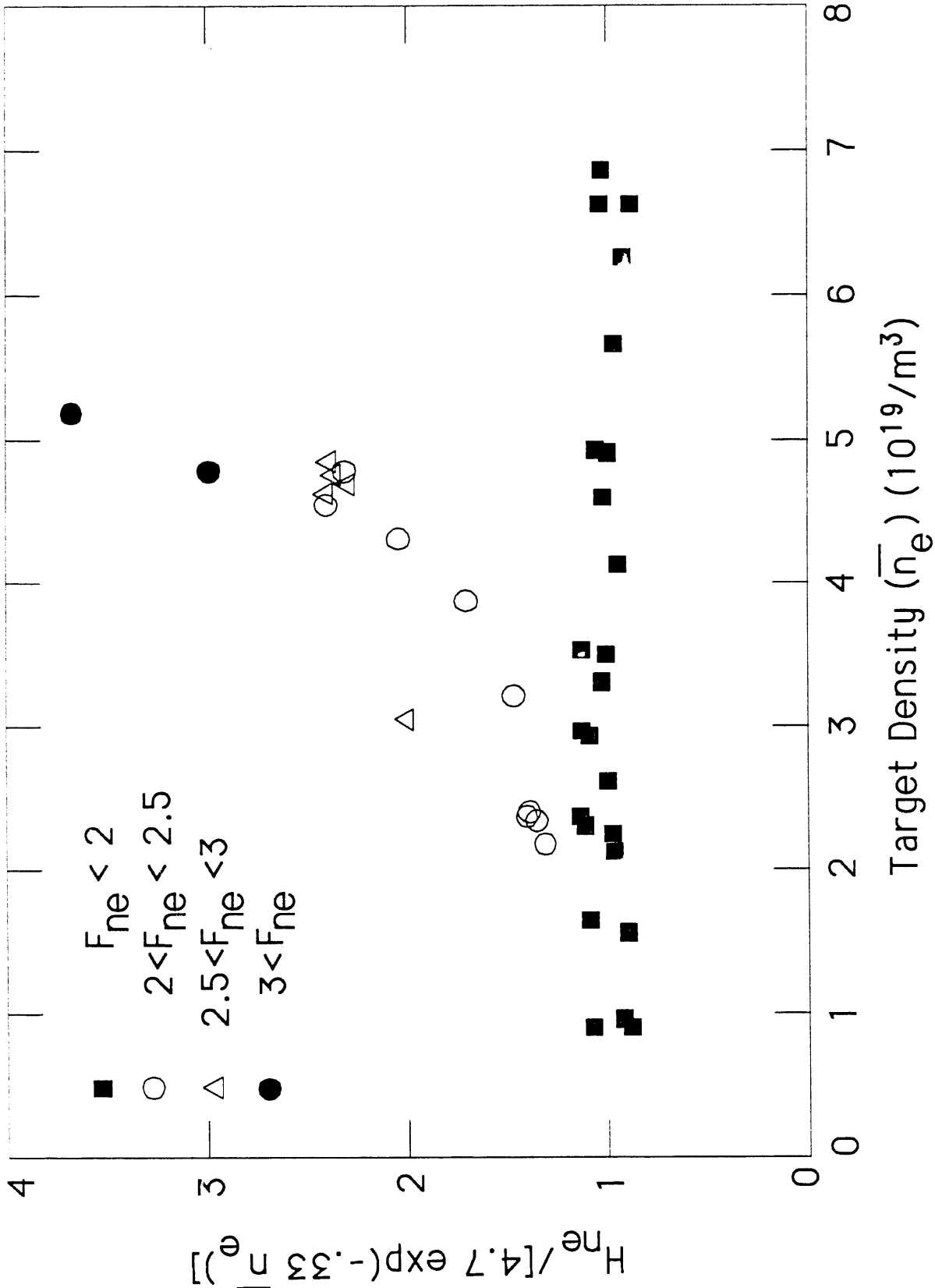
$H_{ne}/[4.7\ \exp(-.33\ \bar{n}_e)]$
Target Density $(\bar{n}_e)$ $(10^{19}/m^3)$
$F_{ne} < 2$
$2 < F_{ne} < 2.5$
$2.5 < F_{ne} < 3$
$3 < F_{ne}$
0
1
2
3
4
5
6
7
8

Fig. 4

EXTERNAL DISTRIBUTION IN ADDITION TO UC-420

Dr. F. Paoloni, Univ. of Wollongong, AUSTRALIA
Prof. M.H. Brennan, Univ. of Sydney, AUSTRALIA
Plasma Research Lab., Australian Nat. Univ., AUSTRALIA
Prof. I.R. Jones, Flinders Univ, AUSTRALIA
Prof. F. Cap, Inst. for Theoretical Physics, AUSTRIA
Prof. M. Heindler, Institut für Theoretische Physik, AUSTRIA
Prof. M. Goossens, Astronomisch Instituut, BELGIUM
Ecole Royale Militaire, Lab. de Phy. Plasmas, BELGIUM
Commission-European, DG. XII-Fusion Prog., BELGIUM
Prof. R. Boucique, Rijksuniversiteit Gent, BELGIUM
Dr. P.H. Sakanaka, Instituto Fisica, BRAZIL
Instituto De Pesquisas Espaciais-INPE, BRAZIL
Documents Office, Atomic Energy of Canada Ltd., CANADA
Dr. M.P. Bachynski, MPB Technologies, Inc., CANADA
Dr. H.M. Skarsgard, Univ. of Saskatchewan, CANADA
Prof. J. Teichmann, Univ. of Montreal, CANADA
Prof. S.R. Sreenivasan, Univ. of Calgary, CANADA
Prof. T.W. Johnston, INRS-Energie, CANADA
Dr. R. Bolton, Centre canadien de fusion magnétique, CANADA
Dr. C.R. James,, Univ. of Alberta, CANADA
Dr. P. Lukac, Komenskeho Universzita, CZECHOSLOVAKIA
The Librarian, Culham Laboratory, ENGLAND
Library, RS1, Rutherford Appleton Laboratory, ENGLAND
Mrs. S.A. Hutchinson, JET Library, ENGLAND
P. Mähönen, Univ. of Helsinki, FINLAND
C. Mouttet, Lab. de Physique des Milieux Ionisés, FRANCE
J. Radet, CEN/CADARACHE - Bat 506, FRANCE
Ms. C. Rinni, Univ. of Ioannina, GREECE
Dr. T. Mual, Academy Bibliographic Ser , HONG KONG
Preprint Library, Hungarian Academy of Sci., HUNGARY
Dr. B. Das Gupta, Saha Inst. of Nuclear Physics, INDIA
Dr. P. Kaw, Inst. for Plasma Research, INDIA
Dr. P. Rosenau, Israel Inst. of Technology, ISRAEL
Librarian, International Center for Theo Physics, ITALY
Miss C. De Palo, Associazione EURATOM-ENEA , ITALY
Dr. G. Grosso, Istituto di Fisica del Plasma, ITALY
Dr. H. Yamato, Toshiba Res & Devel Center, JAPAN
Prof. I. Kawakami, Atomic Energy Res.Inst., JAPAN
Prof. K. Nishikawa, Hiroshima Univ., JAPAN
Director, Japan Atomic Energy Research Inst., JAPAN
Prof. S. Itoh, Kyushu Univ., JAPAN
Data and Planning Center, Nagoya Univ., JAPAN
Prof. S. Tanaka, Kyoto Univ., JAPAN
Library, Kyoto Univ., JAPAN
Prof. N. Inoue, Univ. of Tokyo, JAPAN
S. Mori, Technical Advisor, JAERI, JAPAN
O. Mitarai, Kumamoto Inst. of Technology, JAPAN
H. Jeong, Korea Advanced Energy Research Inst., KOREA
Prof. D.I. Choi, The Korea Adv. Inst. of Sci. & Tech., KOREA
Prof. B.S. Liley, Univ. of Waikato, NEW ZEALAND
Inst. of Plasma Physics, PEOPLE'S REPUBLIC OF CHINA
Librarian, Inst. of Physics, PEOPLE'S REPUBLIC OF CHINA
Library, Tsinghua Univ., PEOPLE'S REPUBLIC OF CHINA
Z. Li, S.W. Inst Physics, PEOPLE'S REPUBLIC OF CHINA
Prof. J.A.C. Cabral, Instituto Superior Tecnico, PORTUGAL
Dr. O. Petrus, AL I CUZA Univ., ROMANIA
Dr. J. de Villiers, Fusion Studies, AEC, S. AFRICA
Prof. M.A. Hellberg, Univ. of Natal, S. AFRICA
C.I.E.M.A.T, Fusion Division Library, SPAIN
Dr. L. Stenflo, Univ. of UMEA, SWEDEN
Library, Royal Inst. of Technology, SWEDEN
Prof. H. Wilhelmson, Chalmers Univ. of Tech., SWEDEN
Centre Phys. Des Plasmas, Ecole Polytech, SWITZERLAND
Bibliotheek, Inst. Voor Plasma-Fysica, THE NETHERLANDS
M. Durgut, Vice Chairman, Middle East Tech. Univ., TURKEY
Dr. D.D. Ryutov, Siberian Branch of Academy of Sci., USSR
Dr. G.A. Eliseev, Kurchatov Inst., USSR
Librarian, The Ukr.SSR Academy of Sciences, USSR
Dr. L.M. Kovrizhnykh, Inst. of General Physics, USSR
Kernforschungsanlage GmbH, Zentralbibliothek, W. GERMANY
Bibliothek, Inst. Für Plasmaforschung, W. GERMANY
Prof. K. Schindler, Ruhr-Universität Bochum, W. GERMANY
Dr. F. Wagner, (ASDEX), Max-Planck-Institut, W. GERMANY
Librarian, Max-Planck-Institut, W. GERMANY
Prof. R.K. Janev, Inst. of Physics, YUGOSLAVIA

END

DATE FILMED

2/03/92